(2) The β-structure possesses the space group $P2_1/n$ (Fig. 6(*b*)).

$10\bar{1}$ is not a space-group absence on either of these arrangements. Intensity calculations, on the basis of the same chain configuration as in the α-structure, show that in structure (1) $10\bar{1}$ has a low calculated intensity requiring more than one quarter of the total crystallites to have the β-structure in the rubbery specimens, and more than one half in the cold drawn specimens. This is not acceptable because such a large proportion would affect the relative intensities of other reflections as between the rubbery and the cold drawn specimens, whereas in fact only $10\bar{1}$ has been observed to change intensity appreciably. In structure (2), $10\bar{1}$ has a large calculated intensity, requiring only 1/20 of the crystallites to have the β-form; this would not affect the other intensities appreciably: in this proportion no other $h0l$ (h odd) reflections would be strong enough to be visible on the photographs. On theoretical grounds the $P2_1/n$ space group is as likely as $P2_1/a$ since the A and B molecules have identical environments. The C=O dipole distance is 3·16 Å, the same as in the α-structure, 3·17 Å, so that the packing of the chains is similar in this respect and the $P2_1/n$ structure would be expected to have some measure of stability. It has therefore been accepted as the most likely for the β-form.

Specimens of pure PEA of moderate molecular weight and of PEA lightly linked with hexamethylene diisocyanate contain a third crystalline form (γ) in the unstretched state which, on cold drawing to give an oriented fibre, is converted into the α-structure. The γ-form shows three very strong equatorial reflections of combined intensity equal to the two strong reflections, 110 and 020, of the α-structure. Two of these reflections have the same spacings as 110 and 020, the third slightly greater than 110, as if the 110 reflection were split into two reflections of roughly equal intensity. PES can also occur in a second crystalline form in the unoriented state.

The authors wish to express their thanks to Drs D. R. Holmes and E. R. Howells, and Mr R. P. Palmer, of these laboratories, for many helpful discussions.

References

ALLEN, P. W. & SUTTON, L. E. (1950). *Acta Cryst.* **3**, 51.

BROWN, C. J. & CORBRIDGE, D. E. C. (1954). *Acta Cryst.* **7**, 711.

BUNN, C. W. & GARNER, E. V. (1947). *Proc. Roy. Soc.* A, **189**, 39.

CARPENTER, G. B. & DONOHUE, J. (1950). *J. Amer. Chem. Soc.* **72**, 2315.

DAUBENY, R. DE P., BUNN, C. W. & BROWN, C. J. (1954). *Proc. Roy. Soc.* **226**, 531.

FULLER, C. S. & ERICKSON, C. L. (1937). *J. Amer. Chem. Soc.* **59**, 344.

FULLER, C. S. & FROSCH, C. J. (1939*a*). *J. Phys. Chem.* **43**, 323.

FULLER, C. S. & FROSCH, C. J. (1939*b*). *J. Amer. Chem. Soc.* **61**, 2575.

FULLER, C. S. (1940). *Chem. Rev.* **26**, 143.

GRENVILLE-WELLS, H. J. (1955). *Acta Cryst.* **8**, 512.

JEFFREY, G. A. & DOUGILL, M. W. (1953). *Acta Cryst.* **6**, 831.

SCHOON, T. (1938). *Z. Phys. Chem.* B, **39**, 385.

VIERVOLL, H. & ØGRIM, O. (1949). *Acta Cryst.* **2**, 277.

Acta Cryst. (1962). **15**, 113

Experimental Determination of Order Phenomena in Liquids and Amorphous Solids

BY H. MENDEL*

Koninklijke/Shell-Laboratorium, Amsterdam
(Shell Internationale Research Maatschappij N.V.)

(*Received* 20 *March* 1961)

A study has been made to determine with what accuracy information can be obtained about order phenomena in liquids and amorphous solids by means of X-ray diffraction. It is shown that with proper experimental conditions and a suitable evaluation of the X-ray intensities, dispensing with sharpening of intensities and with the concept of point atoms, very reliable distribution curves can be obtained, showing no spurious effects near the origin. This method has been tested with good results for cyclohexane, benzene and vitreous silica.

Introduction

It was first shown by Debye (1915) and Ehrenfest (1915), that a regular crystalline arrangement is not essential for the production of diffraction effects. Debye (1925, 1927) later, in a paper on the diffraction of X-rays by gases, introduced the idea of a probability function, expressing the probability of the occurrence of any given interatomic distance. Similar ideas were put forward by Zernike & Prins (1927) in a very

* Present address: Unilever Research Laboratorium, Vlaardingen.

important paper, laying the foundations for the interpretation of diffraction patterns of liquids. They showed how to apply Fourier's integral theorem to the determination of the distribution function of the atoms from the observed diffraction pattern. Since then practically all research on the structure of liquids has been based on their method, which makes use of the concept of point atoms throughout. In the case of liquids containing more than one kind of atom, special difficulties are encountered (see next section).

As X-ray diffraction measurements give information only about the arrangement of electrons, the concept of electron density is used throughout this paper. The measured intensities are a direct function of this quantity and therefore it is physically preferable to deduce the distribution function, and to interpret it quantitatively, directly in terms of electron density, without a transformation to point atoms.

The distribution function as deduced by Zernike & Prins is given by

$$4\pi r^2[\varrho(r)-\varrho_0] = (2r/\pi)\int_0^\infty si(s)\sin sr\,ds \qquad (1)$$

with:

ϱ_0 = average number of atoms per unit volume;
$\varrho(r)$ = radial atomic density;
$i(s)$ = $(I(s)/f^2)-1$ where $I(s)$ is the scattered intensity on an absolute scale and f is the atomic scattering factor;
s = $4\pi\sin\theta/\lambda$ where 2θ is the angle between scattered and primary beam and λ is the wave length.

Equation (1) is strictly valid for monoatomic liquids. Debye (1925, 1927) has extended the treatment to diatomic molecules and Menke (1932) has considered the general case of molecules of any form. Here, however, it is necessary to know their structure, which is often a serious drawback.

Another disadvantage of this method is the use of 'sharpened' intensities, e.g. I/f^2. This often gives rise to serious diffraction ripples in the Fourier transform and may thus obscure the distribution function. In order to diminish these diffraction effects, a convergence factor (van Panthaleon van Eck *et al.*, 1957, 1958), e.g. $\exp[-as^2]$, is sometimes introduced. But this means a transformation of the actual atoms to Gaussian atoms and it is doubtful if much is to be gained by doing this. For liquids containing more than one kind of atom, an 'average' scattering curve (Morgan & Warren, 1938; Warren *et al.*, 1936; Brady, 1958) has to be introduced to obtain the sharpened intensities. This is justified only if the ratio of the different atomic scattering factors is the same for all s-values which actually is not true.

A very stringent test for the correctness of the distribution function is its slope at low values of r (<1 Å). Starting from the origin, the slope has to be continuous and must be related in a specific manner to the mean volume per atom and the average electron density. In the following sections it is shown how distribution curves of liquids consisting of complex molecules were obtained, showing the predicted slope at the origin.

The distribution function

In view of the close connection between the diffracted intensities in reciprocal space and the electron density in direct space, the latter was taken as the starting point in the following. If $\varrho_T(\mathbf{p})$ is the electron density at $\mathbf{p}$ and $\varrho_T(\mathbf{p}+\mathbf{r})$ at $(\mathbf{p}+\mathbf{r})$, then a distribution function $\sigma_T(r)$ is defined by:

$$\sigma_T(r) = \int\int_{V,A}\varrho_T(\mathbf{p})\varrho_T(\mathbf{p}+\mathbf{r})\,dA\,dV, \qquad (2)$$

where $\int_A dA$ is an integration with respect to the components of $\mathbf{r}$ over the surface of a spherical shell of radius $|\mathbf{r}|$ and origin at $\mathbf{p}$, and $\int_V dV$ is with respect to the components of vector $\mathbf{p}$ over the whole volume of the irradiated sample. The double integral has to be calculated for fixed values of $|\mathbf{r}|$, so in the second integration it is the vector $\mathbf{r}+\mathbf{p}$ that moves over the spherical shell whose centre is at $\mathbf{p}$, for all values of $\mathbf{p}$.

If $\varrho_n(\mathbf{p}+\mathbf{r})$ and $\varrho_m(\mathbf{p}+\mathbf{r})$ are the electron densities at $\mathbf{p}+\mathbf{r}$ due to atom n and m, respectively, equation (2) can be written:

$$\sigma_T(r) = \sum_n\int\int_{V,A}\varrho_n(\mathbf{p})\varrho_n(\mathbf{p}+\mathbf{r})\,dA\,dV + \sum_{n\neq m}\sum\int\int_{V,A}\varrho_n(\mathbf{p})\varrho_m(\mathbf{p}+\mathbf{r})\,dA\,dV \equiv \sigma_a(r)+\sigma(r). \qquad (3)$$

The first integral, summed over all atoms in the irradiated volume, contains intra-atomic distances while the second integral contains all interatomic distances.

Therefore, two distinct terms can be distinguished: $\sigma_a(r)$ gives all intra-atomic distances and can be calculated from the scattering curves; $\sigma(r)$ contains structural information about the molecules (intramolecular distances) and the liquid itself (intermolecular distances).

It is convenient to introduce the average electron density $\bar{\varrho}$. Then $\varrho(\mathbf{p})=\bar{\varrho}+\Delta\varrho(\mathbf{p})$ and at large enough values of $|\mathbf{r}|$ the time-average value of $\varrho(\mathbf{p}+\mathbf{r})=\bar{\varrho}$. From equation (3) $\sigma(r)$ can now be written:

$$\sigma(r) = \int\int_{V,A}\bar{\varrho}^2\,dA\,dV + \int\int_{V,A}\Delta\varrho(\mathbf{p})\Delta\varrho(\mathbf{p}+\mathbf{r})\,dA\,dV \qquad (4)$$

as cross products of $\bar{\varrho}$ and $\Delta\varrho$ cancel out. By defining

$$\sigma_M(r) \equiv \int\int_{V,A}\Delta\varrho(\mathbf{p})\Delta\varrho(\mathbf{p}+\mathbf{r})\,dA\,dV$$

it is easily shown that

$$\sigma(r) = 4\pi r^2\bar{\varrho}^2 V + \sigma_M(r)\,. \qquad (5)$$

$\sigma_M(r)$ is a measure of the departure of the mean product of electron densities at a distance $|\mathbf{r}|$ apart from the square of the average electron density.

The total coherent scattering from the sample $I_T^c(s)$ is built up from the following components: the scattering due to distances within the same atom, $I_{\text{coh.}}(s)$, the scattering due to order phenomena $I_M(s)$ and, the zero-angle scattering $I_0(s)$. All these intensities can be calculated from the distribution functions:

$$I_T^c(s) = \int_0^\infty \sigma_T(r) \frac{\sin sr}{sr}\, dr;\quad I_{\text{coh.}}(s) = \int_0^\infty \sigma_a(r) \frac{\sin sr}{sr}\, dr;$$

$$I_M(s) = \int_0^\infty \sigma_M(r) \frac{\sin sr}{sr}\, dr;\quad I_0(s) = \int_0^\infty 4\pi r^2 \bar{\varrho}^2 V \frac{\sin sr}{sr}\, dr .$$

Knowledge of $I_M(s)$ would make it possible to calculate $\sigma_M(r)$ by means of a Fourier transform, thus giving experimental evidence of order phenomena:

$$\frac{\pi}{2}\frac{\sigma_M(r)}{r} = \int_0^\infty s I_M(s) \sin sr\, ds . \tag{6}$$

The intensity $I_M(s)$ can be obtained from the following equation:

$$I_T^c(s) = I_{\text{coh.}}(s) + I_M(s) + I_0(s) . \tag{7}$$

$I_T^c(s)$ is the total coherent experimental intensity on an absolute scale and $I_{\text{coh.}}(s)+I_0(s)$ can be calculated. The only problem left is to bring the experimental intensities to absolute scale. In the following the absolute scale is normalized to one atom, namely the scattered intensity of the irradiated sample in absolute scale is divided by the number of atoms in the sample.

Then equation (5) after substitution of equation (6) becomes

$$\frac{\pi}{2}\frac{\sigma(r)}{r} = \int_0^\infty s I_M(s) \sin sr\, ds + 2\pi^2 r (N/V)\bar{z}^2 \tag{8}$$

with $\bar{\varrho} = (N/V)\bar{z}$ where N/V = number of atoms per unit volume and $\bar{z}$ = mean number of electrons per atom. As $I_M(s)$ is experimentally only accessible in a limited s-range, the integration limits $0 \to \infty$ in equation (8) have to be replaced by $s_{\text{min.}} \to s_{\text{max.}}$. There is no objection to this procedure, because at large values of r, $\sigma_M(r)$ becomes zero, owing to the term $\Delta\varrho(\mathbf{p}+\mathbf{r})$ in the definition of $\sigma_M(r)$ (equation (4)). Therefore, as no periodicity occurs in a liquid, the corresponding value of $I_M(s)$, which has to be observed at low values of s, becomes zero and the lower integration limit in equation (8) can be replaced by $s_{\text{min.}}$. Also, at high values of s, corresponding with r-values smaller than the atomic radii, $I_M(s)$ will become zero if the atoms do not overlap, all intra-atomic contributions being given by $I_{\text{coh.}}(s)$.

Determination of $I_M(s)$

As shown in the previous section, it would be possible to calculate directly $\sigma(r)$ if the $I_M(s)$ were known. Experiment, however, gives the total diffracted intensity on an arbitrary scale, from which $I_M(s)$ has to be deduced. This total observed scattered intensity on absolute scale, $I_T(s)$ from the sample is:

$$I_T(s) = I_M(s) + I_{\text{coh.}}(s) + I_{\text{inc.}}(s) + I_{\text{fl.}}(s) . \tag{9}$$

$I_M(s)$: scattering due to order phenomena in the liquid;
$I_{\text{coh.}}(s)+I_{\text{inc.}}(s)$: the coherent and incoherent atomic background scattering;
$I_{\text{fl.}}(s)$: fluorescence radiation.

$I_M(s)$ can be determined if all other quantities in equation (9) are known on an absolute scale. $I_{\text{coh.}}(s)$ and $I_{\text{inc.}}(s)$ can be calculated on this scale from the chemical composition of the sample. $I_{\text{fl.}}(s)$, the fluorescence radiation, is a parasitic radiation for which it is extremely difficult to correct, because the sensitivity of the photographic film varies with the wave length and the tabulated fluorescence yields are inaccurate. Its intensity may be comparable to $I_M(s)$ and can therefore on no account be neglected. Generally, however, the wave length of the fluorescence radiation differs considerably from the incident radiation and thus the former can be eliminated by selective absorption. In this case equation (9) becomes:

$$I_M(s) = I_T(s) - [I_{\text{coh.}}(s) + I_{\text{inc.}}(s)] . \tag{10}$$

It now remains to convert the experimental intensity $I_e(s)$—after correction for polarization and absorption —from an arbitrary scale into the absolute scale by means of the scaling factor α (Krogh-Moe, 1956; Norman, 1957), namely $I_T(s) \equiv \alpha I_e(s)$. Once α is known, calculations become straightforward.

If there is no overlapping of the electron shells of atoms, interatomic distances r that approach zero do not occur. Therefore

$$\left[\int_V \varrho_n(\mathbf{p})\varrho_m(\mathbf{p}+\mathbf{r})\, dV\right]_{r\to 0} \to 0$$

on substituting $dA = d(4\pi r^2)$ into equation (3) and differentiating with respect to r gives

$$\left[d\left(\frac{\sigma(r)}{r}\right)\Big/ dr\right]_{r\to 0} \to 0 .$$

This condition, on differentiation of equation (8) with respect to r, gives:

$$\int_0^\infty s^2 I_M(s)\, ds = -2\pi^2 (N/V)\bar{z}^2 . \tag{11}$$

Substitution of equation (10) into equation (11) and replacement of $I_T(s)$ by $\alpha I_e(s)$ gives, after rearrangement:

$$\alpha = \frac{\int_0^\infty s^2[(I_{\text{coh.}}(s)+I_{\text{inc.}}(s)]ds - 2\pi^2(N/V)\bar{z}^2}{\int_0^\infty s^2 I_e(s)\,ds}. \quad (12)$$

In practice the upper integration limit has to be replaced by the highest experimental s-value. As shown by Krogh-Moe (1956) and Norman (1957), a rapid convergence of α is obtained at s-values which are easily accessible experimentally, provided overlap can be neglected. This latter condition is nearly always fulfilled for atoms separated by the sum of their van der Waals radii, whereas overlap can occur at smaller interatomic distances, e.g. bond distances. If the assumption is made that overlap can be described as a superposition of spherical atoms, then its contribution to $I_M(s)$ will be:

$$I_{\text{ov.}}(s) = \int_0^\infty \left[\iint_{VA}\sum_{m\neq n} \varrho_n(\mathbf{p})\,\varrho_m(\mathbf{p}+\mathbf{r})\,dA\,dV \right] \frac{\sin sr}{sr}\,dr \quad (13)$$

which expression can be evaluated for spherical atoms m and n if the bond distances are known. In this case the expression for the scaling factor becomes:

$$\alpha = \frac{\int_0^s s^2[I_{\text{coh.}}(s)+I_{\text{inc.}}(s)]ds - 2\pi^2\frac{N}{V}\bar{z}^2 + \int_0^s s^2 I_{\text{ov.}}(s)\,ds}{\int_0^s s^2 I_e(s)\,ds}. \quad (14)$$

In the case of liquids containing more than one kind of atom, it can easily be shown that:

$I_{\text{coh.}}(s) \equiv \overline{f^2}(s)$ with $\overline{f^2} = \sum_1^p m_p f_p^2$; m_p = mole fraction of atoms p; f_p = atomic form factor of atom p;

$I_{\text{inc.}}(s) = \sum_1^p m_p I_{\text{inc.}}^p(s)$; $I_{\text{inc.}}^p(s)$ = incoherent scattering of atom p;

$\bar{z} = \sum_1^p m_p z_p$; z_p = number of electrons of atom p.

Discussion of errors

The reliability of the experimental distribution curves is governed by the accuracy of $I_M(s)$. As $I_M(s)$ is obtained as the difference between $\alpha I_e(s)$ and the sum of the coherent and incoherent scattering, relatively small errors in anyone of these can produce a relatively large error in $I_M(s)$. The most important errors are the systematic ones, which will be considered first.

Systematic errors in the background arise from the use of incorrect atomic scattering curves. In the calculation of the scaling factor consistent results were obtained only by using scattering curves calculated from the most recent self-consistent-field data (Berghuis *et al.*, 1955), including—if necessary—correction for dispersion. Possible systematic errors in the incoherent scattering can usually be neglected as their contribution to the total background is small.

Systematic errors in the experimental intensities can arise when the recorded film densities are converted into intensities. This is usually done by taking as zero level the non-exposed part of the film; but a serious error is introduced when the zero level of the exposed part of the film is different (e.g. fluorescence radiation, extraneous scattering). If we suppose, for the sake of the argument, that the difference in zero level is a constant Δ, independent of s, then the true experimental intensities $I_e(s)$ and the measured intensities $I_e^m(s)$ are connected by the following formula

$$I_e(s) = I_e^m(s) + \Delta P^{-1}A^{-1} \quad (15)$$

with P^{-1} and A^{-1} as polarization and absorption correction, respectively. This introduces an error $\delta\alpha$ in the scaling factor of the measured intensities. The expression for the distribution function now becomes:

$$\int_0^s sI_M(s)\sin sr\,ds = \int_0^s sI_M^m(s)\sin sr\,ds + \delta\alpha\int_0^s sI_e^m(s)\sin sr\,ds + \alpha\Delta\int_0^s sA^{-1}P^{-1}\sin sr\,ds. \quad (16)$$

The last-mentioned two integrals are given in Fig. 1, calculated for water. Their most characteristic feature is a very high maximum at low values of r and a diffraction ripple at higher r-values. The combined effects of these two curves lead to a peak at $r < 1$ Å; therefore the occurrence of such a peak may be an indication of

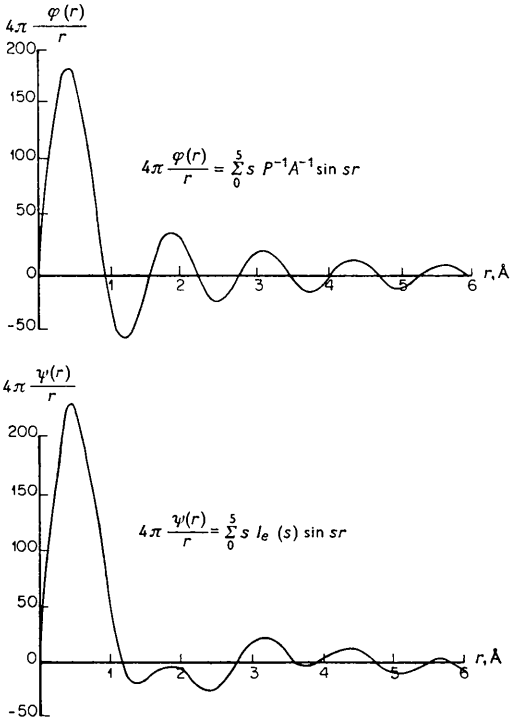

Fig. 1. False details, superimposed on distribution curves as a result of errors in zero level.

a systematic error. The diffraction ripple with wave length $\lambda \sim 1{\cdot}2$ Å is caused by the breaking-off effect at $s=5$.

The only random errors considered are those in the readings of the microphotometer diagram. If here an error δ is assumed, then the quadratic deviation u^2 of the distribution function $\pi/2(\sigma_M(r)/r)$ is:

$$u^2 = \int_0^s [\alpha\delta]^2 s^2 \sin^2 sr\,ds;$$

at large values of r: $u^2 \approx \frac{1}{6}[\alpha\delta]^2 s^3$.

This error is rather small and checks well with the experimentally determined difference between distribution curves based on different photographs of the same sample.

Therefore a smooth continuous slope of the distribution curve near the origin coupled with the absence of spurious diffraction ripples is a direct check on its reliability, as this region of low r-values is very sensitive towards systematic errors.

Experimental technique

The technique (van Panthaleon van Eck *et al.*, 1957, 1958) adopted is a version of that of Katzoff (1934) and that of Morgan & Warren (1938). The specimen is a liquid jet, centred in a cylindrical camera and irradiated with a monochromatic X-ray beam. In order to eliminate extraneous scattering, helium is circulated through the camera and the film is protected against fluorescence radiation by selective filters. For the samples investigated—SiO_2, C_6H_6, C_6H_{12}—Kel-F foils (i.e. $[-(C_2F_3Cl)-]_n$) were used. The liquid circulates in a closed system making it possible to obtain long exposure times with a limited amount of liquid (~ 30 ml.). All photographs were taken with monochromatized Cu $K\alpha$ radiation. The film densities were converted by an automatic microphotometer into intensities, which were corrected for polarization and absorption to give the experimental intensities. The diameter of the samples used was 0·3–0·4 mm.

Results

(a) *Cyclohexane*

The distribution curves for cyclohexane are given in Fig. 2(*a*) and 2(*b*). The scaling factor α was calculated for different values of the upper integration limit s_m with a sampling interval of $\Delta s = \frac{1}{8}$. In the calculation of the background scattering, hydrogen atoms were included. As can be seen in Table 1 good constancy is obtained at s-values $> 6\frac{1}{2}$; thus the distribution curve obtained will be reliable. In Fig. 2(*b*) the function $\sigma(r)/r^2$ is given, showing clearly that at higher r-values the actual distribution becomes equal to a statistical one.

Table 1. *Convergence of scaling factor for cyclohexane*

s	α
5	0·302
$5\frac{1}{2}$	0·300
6	0·300
$6\frac{1}{2}$	0·305
7	0·307
$7\frac{1}{2}$	0·307

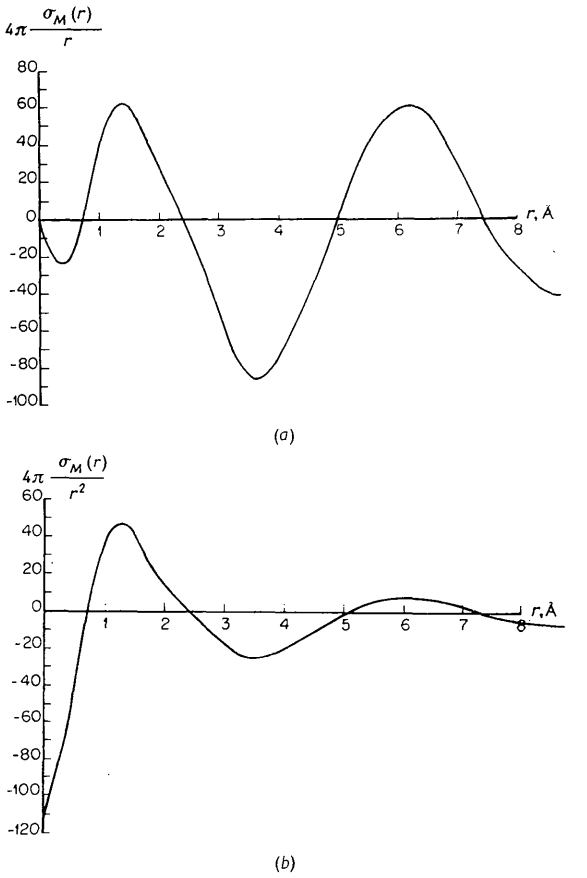

Fig. 2. (*a*) Distribution curve $4\pi\sigma_M(r)/r$ of cyclohexane at 18° C. (*b*) Distribution curve $4\pi\sigma_M(r)/r^2$ of cyclohexane at 18 °C.

(b) *Benzene*

The distribution curve for benzene is given in Fig. 3. In scaling the experimental intensities, the sampling interval Δs was taken as $\frac{1}{16}$, because of the sharpness of the intensity peaks. In the benzene molecule,

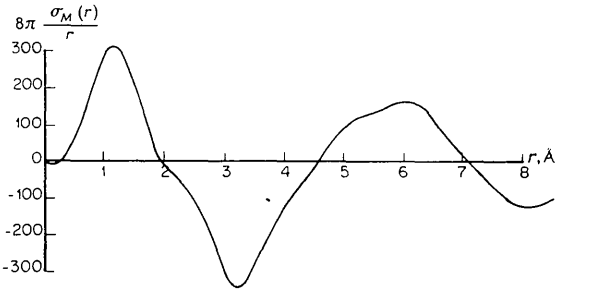

Fig. 3. Distribution curve of benzene at 18 °C.

overlap of atoms separated by bonding distances will occur, so the overlap correction has to be included in calculating the scaling factor (equation (14)). As the structure of the benzene molecule is well-known, calculation of the intensities $I_{ov.}(s)$—equation (13)—is straightforward, being based on all intramolecular atomic distances including hydrogen.

Table 2. *Convergence of scaling factor for benzene*

s_m	α_1	α_2
$5\frac{1}{2}$	0·477	0·498
6	0·478	0·494
$6\frac{1}{2}$	0·482	0·496
7	0·488	0·502
$7\frac{1}{2}$	0·495	0·503
8	0·501	0·502

In Table 2, α_1 is the scaling factor deduced without overlap correction, whereas the latter is included in the calculation of α_2. As can be seen, constancy of the scaling factor is only obtained by including the overlap correction. The distribution curve $\sigma_M(r)/r$ is calculated without this correction; therefore, overlap is expected to show up. This is confirmed by the slope of the curve near the origin, indicating that right from the beginning ($r=0$) the contribution to $\sigma(r)/r$ is different from zero.

(*c*) *Vitreous* SiO_2

The distribution curve for vitreous silica is given in Fig. 4. The intensities were sampled with an interval of $\Delta s=\frac{1}{8}$. Here again the overlap correction has to be included in the calculation of the scaling factor in order to obtain convergence. This correction was calculated for the silicon–oxygen tetrahedron, based

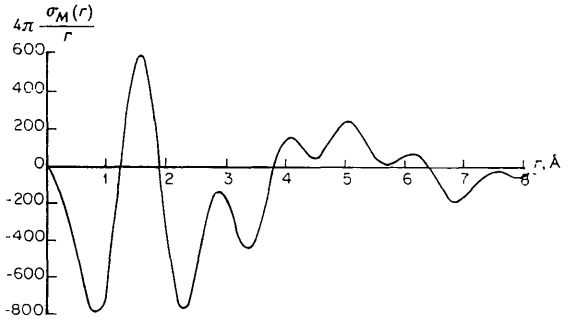

Fig. 4. Distribution curve of vitreous SiO_2.

on the known Si–O and O · · · O distances. The distribution curve $\sigma_M(r)/r$ is again calculated without correction for overlap, which therefore shows up near the origin, where the curve is slightly convex. A detailed quantitative interpretation of the first part of this distribution function is given by Heemskerk (1958).

Discussion

As shown above, the method described has made it possible to obtain distribution curves of liquids and amorphous solids with the theoretically expected slope near the origin. This is further demonstrated for cyclohexane by calculating $\sigma(r)/r$ (Fig. 5). As all intra-atomic contributions have been subtracted, the curve has to be zero at very low r-values and then increase with a smooth and continuous slope towards higher r-values. That this is indeed realized is due to the elimination of diffraction ripples and spurious waves, which both exert their maximum influence in this region. Diffraction ripples have been removed by using a convergent Fourier series which was obtained

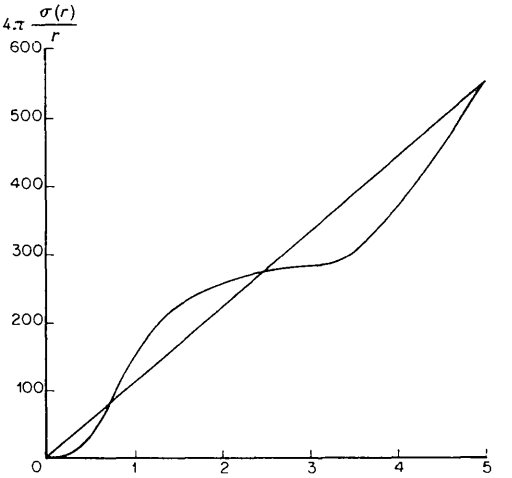

Fig. 5. Distribution curve $4\pi\sigma(r)/r$ of cyclohexane at 18 °C.

from 'unsharpened' intensities (not divided by f^2). This is especially of advantage in polyatomic liquids, as here division by f^2 is not possible and an 'effective' atomic scattering curve has to be assumed. Spurious waves do not occur because the proper atomic scattering curves were used and the scaling factor was accurately determined, including—if necessary—an overlap correction. The latter proved to be necessary in our experiments with molecules containing small bonding distances.

The distribution curves obtained can be interpreted quantitatively in the usual way by a comparison of experimental and calculated peak values. This is shown in detail by Heemskerk (1958).

It is a pleasure to thank Mrs E. G. M. de Hertog-Zaat and Mrs J. P. M. A. van Asselt-Ekkers for doing most of the experimental work and for their help in carrying out numerous calculations. I am further indebted to Dr J. Beintema for his stimulating criticism.

References

Berghuis, J., Haanappel, IJ. M., Potters, M., Loopstra, B. O., MacGillavry, C. H. & Veenendaal, A. L. (1955). *Acta Cryst.* **8**, 478.
Brady, G. W. (1958). *J. Chem. Phys.* **28**, 464.
Debye, P. (1915). *Ann. Phys. Lpz.* **46**, 809.

DEBYE, P. (1925). *J. Math. & Phys.* **4**, 153.
DEBYE, P. (1927). *Phys. Z.* **28**, 135.
EHRENFEST, P. (1915). *Proc. Ned. Akad. Wet.* **17**, 1132, 1184.
HEEMSKERK, J. (1958). Thesis. Leiden.
KATZOFF, S. (1934). *J. Chem. Phys.* **2**, 841.
KROGH-MOE, J. (1956). *Acta Cryst.* **9**, 951.
MENKE, H. (1932). *Phys. Z.* **33**, 593.
MORGAN, J. & WARREN, B. E. (1938). *J. Chem. Phys.* **6**, 666.
NORMAN, N. (1957). *Acta Cryst.* **10**, 370.
VAN PANTHALEON VAN ECK, C. L., MENDEL, H. & BOOG, W. (1957). *Discussions Faraday Soc.* **24**, 200.
VAN PANTHALEON VAN ECK, C. L., MENDEL, H. & FAHRENFORT, J. (1958). *Proc. Roy. Soc.* (London) A **247**, 472.
WARREN, B. E., KRUTTER, H. & MORNINGSTAR, O. (1936). *J. Amer. Ceramic Soc.* **19**, 202.
ZERNIKE, F. & PRINS, J. A. (1927). *Phys. Z.* **41**, 184.

Acta Cryst. (1962). **15**, 119

The Direct Determination of Molecular Structure: The Crystal Structure of Himbacine Hydrobromide at −150 °C

BY J. FRIDRICHSONS AND A. MCL. MATHIESON

Division of Chemical Physics, Chemical Research Laboratories, C.S.I.R.O., Melbourne, Australia

(*Received* 15 *March* 1961)

Himbacine hydrobromide monohydrate, $C_{22}H_{35}O_2N.HBr.H_2O$, crystallizes in the orthorhombic system,

$$a = 6{\cdot}678,\ b = 12{\cdot}670,\ c = 26{\cdot}317\ \text{Å}$$

measured at *circa* −150 °C., the space group being $P2_12_12_1$ with $Z = 4$. Starting with only the empirical formula, the structure was solved by means of zero-layer projections and first-layer generalized projections, image-seeking methods being discarded in favour of direct ϱ_0 and $\Delta\varrho$ syntheses. The absolute configuration was then established by reference to the anomalous dispersion of the Br atom.

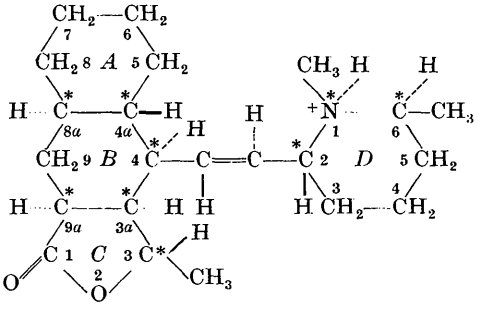

The organic ion whose systematic name is *trans*-1-[2-(1,6-dimethyl piperidyl)]-2-[4-(1-oxo-3-methyl-dodecahydronaphtho [2,3-c] furanyl)]-ethylene has 9 asymmetric centres (starred atoms). The rings *A*, *B* and *D* are in the chair conformation. Between *A* and *B* there is a *trans*-junction, between *B* and *C* a *cis*-junction. The piperidine substituent at 6 is axial, those at 1 and 2 equatorial; the naphthofuran substituent at 3*a* is axial, those at 4 and 9*a* equatorial. Bond lengths and angles are presented, those in the γ-lactone system being discussed in more detail.

The experimental conditions of the analysis were selected to reduce the number of unobserved terms to a minimum and the influence of this factor on the process of analysis is discussed.

When the X-ray analysis was initiated in May 1959, himbacine was regarded from the chemical viewpoint as the most important of the alkaloids isolated from *Himantandra* (*Galbulimima*) species (Brown, Drummond, Fogerty, Hughes, Pinhey, Ritchie & Taylor, 1956) in that it appeared to provide a structural key to certain of the related alkaloids. Thus, a solution of the structure and the elucidation of its stereochemistry in detail could be of considerable assistance in the correlation of the associated group of compounds and in relating himbacine to other natural products, especially if the absolute rather than the relative configuration could be defined.

Drs E. Ritchie, W. C. Taylor and J. T. Pinhey, of the Department of Chemistry in the University of Sydney, who were investigating the structures of